Article

Multilabeled Pyrene-Functionalized 2'-Amino-LNA Probes for Nucleic Acid Detection in Homogeneous Fluorescence Assays

Patrick J. Hrdlicka, B. Ravindra Babu, Mads D. Srensen, Niels Harrit, and Jesper Wengel

J. Am. Chem. Soc., **2005**, 127 (38), 13293-13299• DOI: 10.1021/ja052887a • Publication Date (Web): 02 September 2005

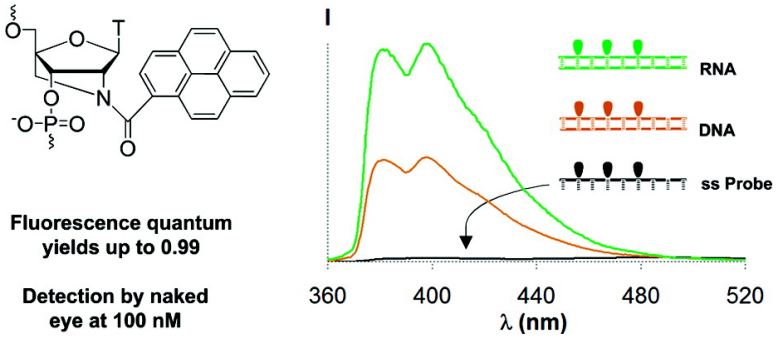

More About This Article

Additional resources and features associated with this article are available within the HTML version:

- Supporting Information
- Links to the 19 articles that cite this article, as of the time of this article download
- Access to high resolution figures
- Links to articles and content related to this article
- Copyright permission to reproduce figures and/or text from this article

View the Full Text HTML

J|A|C|S
ARTICLES
Published on Web 09/02/2005

Multilabeled Pyrene-Functionalized 2′-Amino-LNA Probes for Nucleic Acid Detection in Homogeneous Fluorescence Assays

Patrick J. Hrdlicka,[†] B. Ravindra Babu,[†] Mads D. Sørensen,[‡] Niels Harrit,[§] and Jesper Wengel*,[†]

Contribution from the Nucleic Acid Center,[||] Department of Chemistry, University of Southern Denmark, DK-5230 Odense M, Denmark, and Department of Chemistry, University of Copenhagen, Universitetsparken 5, DK-2100 Copenhagen, Denmark, and Nano-Science Center, University of Copenhagen, Universitetsparken 5, DK-2100 Copenhagen, Denmark

Received May 3, 2005; E-mail: jwe@chem.sdu.dk

Abstract: Homogeneous fluorescence assays for detection of nucleic acids are widely used in biological sciences. Typically, probes such as molecular beacons that rely on distance-dependent fluorescence quenching are used for such assays. Less attention has been devoted to tethering a single kind of fluorophores to oligonucleotides and exploiting hybridization-induced modulation of fluorescence intensity for nucleic acid detection. Herein, thermal denaturation experiments and fluorescence properties of oligodeoxyribonucleotides containing one or more 2′-*N*-(pyren-1-yl)carbonyl-2′-amino-LNA monomer(s) **X** are described. These pyrene-functionalized 2′-amino-LNAs display large increases in thermal stability against DNA/RNA complements with excellent Watson−Crick mismatch discrimination. Upon duplex formation of appropriately designed 2′-*N*-(pyren-1-yl)carbonyl-2′-amino-LNA probes and complementary DNA/RNA, intensive fluorescence emission with quantum yields between 0.28 and 0.99 are observed. Quantum yields of such magnitudes are unprecedented among pyrene-labeled oligonucleotides. Molecular modeling studies suggest that the dioxabicyclo[2.2.1]heptane skeleton and amide linkage of monomer **X** fix the orientation of the pyrene moiety in the minor groove of a nucleic acid duplex. Interactions between pyrene and nucleobases, which typically lead to quenching of fluorescence, are thereby reduced. Duplexes between multiple modified probes and DNA/RNA complements exhibit additive increases in fluorescence intensity, while the fluorescence of single stranded probes becomes increasingly quenched. Up to 69-fold increase in fluorescence intensity (measured at $\lambda_{em} = 383$ nm) is observed upon hybridization to DNA/RNA. The emission from duplexes of multiple modified probes and DNA/RNA at concentrations down to less than 500 nM can easily be seen by the naked eye using standard illumination intensities.

Introduction

Homogeneous fluorescence assays (i.e., all-in-solution assays) are widely used for detection of nucleic acids and have been successfully applied for (a) real-time monitoring of PCR,[1] (b) real-time in vivo imaging of RNA,[2] (c) detection of single nucleotide polymorphisms,[3] (d) study of RNA folding[4−5] and (e) detection of acceptor sites for antisense oligonucleotides.[6] Probes for homogeneous fluorescence assays[1,7−8] must generate a measurable hybridization-induced difference in fluorescence intensity since excess probe cannot be washed out. The simplest probes are small molecules such as, e.g., ethidium bromide or cyanine dyes that become fluorescent upon intercalation into double stranded DNA.[9,10] A significant limitation of these probes is their unspecific binding to double stranded DNA.[11] Specific detection of nucleic acids is realized by tethering reporter groups to single stranded oligonucleotides (ONs) and taking advantage of the Watson−Crick base-pairing rules. The fluorescence of cyanine dyes conjugated to ONs[12,13] or peptide nucleic acids (PNAs),[14,15] is known to increase (2−50-fold) upon hybridiza-

* To whom correspondence should be addressed. Tel: (+45) 6550 2510. Fax: (+45) 66158780.
[†] Nucleic Acid Center.
[‡] Department of Chemistry, University of Copenhagen.
[§] Nano-Science Center, University of Copenhagen.
[||] A research center funded by the Danish National Research Foundation for studies on nucleic acid chemical biology.

(1) Wilhelm, J.; Pingoud, A. *ChemBioChem* **2003**, *4*, 1120−1128.
(2) Bratu, D. P.; Cha, B.-J.; Mhlanga, M. M.; Kramer, F. R.; Tyagi, S. *Proc. Natl. Acad. Sci. USA* **2003**, *100*, 13308−13313.
(3) Nakatani, K. *ChemBioChem* **2004**, *5*, 1623−1633.
(4) Bevilacqua, P. C.; Kierzek, R.; Johnson, K. A.; Turner, D. H. *Science* **1992**, *258*, 1355−1358.
(5) Silverman, S. K.; Cech, T. R. *Biochemistry* **1999**, *38*, 14224−14237.
(6) Mahara, A.; Iwase, R.; Sakamoto, T.; Yamaoka, T.; Yamana, K.; Murakami, A. *Bioorg. Med. Chem.* **2003**, *11*, 2783−2790.
(7) Seitz, O. 311−328. In *Highlights in Bioorganic Chemistry: Methods and Applications*; Schmuck, C., Wennemers, H, Eds.; Wiley−VCH Verlag GmbH & Co.: Weinheim, 2004.
(8) Morrison, L. E. *J. Fluoresc.* **1999**, *9*, 187−196.
(9) Glazer, A. N.; Rye, H. S. *Nature* **1992**, *359*, 859−860.
(10) Higuchi, R.; Fockler, C.; Dollinger, G.; Watson, R. *BioTechnology* **1993**, *11*, 1026−1030.
(11) Petty, J. T.; Bordelon, J. A.; Robertson, M. E. *J. Phys. Chem. B* **2000**, *104*, 7221−7227.
(12) Ishiguro, T.; Saitoh, J.; Yawata, H.; Otsuka, M.; Inoue, T.; Sugiura, Y. *Nucleic Acids Res.* **1996**, *24*, 4992−4997.
(13) Privat, E.; Melvin, T.; Merola, F.; Schwelzer, G.; Prodhomme, S.; Asseline, U.; Vigny, P. *Photochem. Photobiol.* **2002**, *75*, 201−210.

tion to DNA or RNA complements. However, sequence- and temperature-dependent high levels of fluorescence of the single stranded probes,[12−16] small hybridization-induced increases in fluorescence intensity[13] or low fluorescence quantum yields of the hybridized complexes[13,14] are observed. The majority of probes for specific detection of nucleic acids rely on distance-dependent fluorescence quenching.[17] Hybridization events, which lead to an increase in fluorophore-quencher distance, result in an increase in fluorescence intensity. Examples of such probes are molecular beacons,[18] Sunrise primers,[19] Taqman probes,[20] or Scorpion primers.[21] Unfortunately, probes utilizing a decrease-of-quenching mechanism may generate false positive signals due to formation of unintended secondary structures or hydrolysis of the probe.[1,8] An alternative strategy for detection of nucleic acids has been to attach a single kind of fluorophore to ONs, and to take advantage of hybridization-induced modulations of fluorescence intensity. Partial success has been accomplished with ONs labeled with fluoresceins,[22−25] Cy3,[26] dansyl,[27] or pyrenes.[28−35] However, none of these probes satisfy all of the following desirable requirements: (a) Enhanced thermal stability of duplexes formed by hybridization to complementary DNA/RNA with good mismatch discrimination, (b) large hybridization-induced increase in fluorescence intensity, (c) generation of brightly fluorescent duplexes[36] and (d) the ability of multiple labeling without reduction in absorption or fluorescence quantum yields, to generate even more fluorescent duplexes. In this paper, thermal denaturation experiments and fluorescence properties of oligodeoxyribonucleotides containing 2′-*N*-(pyren-1-yl)carbonyl-2′-amino-LNA monomer **X** (Figure 1) are described. These probes satisfy all the above-mentioned requirements. Their design and preparation are based on the well-established high-affinity hybridizations of LNA[37−40] and 2′-amino-LNA[41,42] (Figure 1) to DNA/RNA complements, and on our recent efforts focusing on attaching reporter groups to 2′-amino-LNA to generate functional nucleic acid architectures[43−45] with potential application for Ångström-scale chemical engineering.[46]

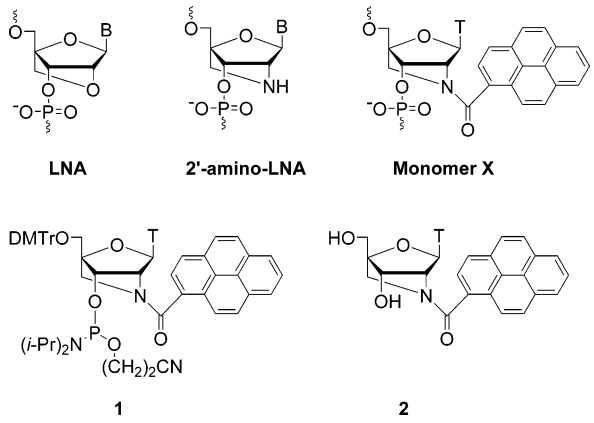

Figure 1. Structures of LNA, 2′-amino-LNA, 2′-*N*-(pyren-1-yl)carbonyl-2′-amino-LNA monomer **X**, phosphoramidite **1** and unprotected nucleoside **2**, T = thymin-1-yl.

Results and Discussion

Synthesis of 2′-*N*-(Pyren-1-yl)carbonyl-2′-amino-LNAs. Synthesis and workup of ONs containing 2′-amino-LNA monomer **X** (Figure 1) was performed using a standard DNA synthesizer following standard protocols except for extended coupling times for phosphoramidite **1**[43,47] (10 min, using 1*H*-tetrazole as catalyst), which resulted in stepwise coupling yields of ∼98% of monomer **X**. 2′-*N*-(Pyren-1-yl)carbonyl-2′-amino-LNAs were purified by reversed-phase HPLC and their composition verified by MALDI-MS analysis (Table S1).[48]

Thermal Stability of Duplexes between 2′-*N*-(Pyren-1-yl)-carbonyl-2′-amino-LNAs and DNA/RNA. The effect on duplex stability upon incorporation of monomer **X** into ONs was evaluated by UV thermal denaturation experiments using medium salt buffer ([Na^+] = 110 mM) and compared to the corresponding unmodified reference duplexes (Table 1). In all cases, the denaturation curves displayed sigmoidal monophasic transitions with a shape similar to that observed for unmodified reference duplexes.[48] Incorporation of a single monomer **X** into mixed sequence 9-mer ONs (**ON1-ON3**) induces large increases in thermal stability of duplexes formed with DNA/RNA com-

(14) Svanvik, N.; Westman, G.; Wang, D.; Kubista, M. *Anal. Biochem.* **2000**, *281*, 26−35.
(15) Köhler, O.; Jarikote, D. V.; Seitz, O. *ChemBioChem* **2005**, *6*, 69−77.
(16) Svanvik, N.; Nygren, J.; Westman, G.; Kubista, M. *J. Am. Chem. Soc.* **2001**, *123*, 803−809.
(17) Johansson, M. K.; Cook, R. M. *Chem. Eur. J.* **2003**, *9*, 3466−3471.
(18) Tyagi, S.; Kramer, F. R. *Nat. Biotechnol.* **1996**, *14*, 303−308.
(19) Nazarenko, I. A.; Bhatnagar, S. K.; Hohman, R. J. *Nucleic Acids Res.* **1997**, *25*, 2516−2521.
(20) Gelmini, S.; Orlando, C.; Sestini, R.; Vona, G.; Pinzani, P.; Ruocco, L.; Pazzagli, M. *Clin. Chem.* **1997**, *43*, 752−758.
(21) Whitcombe, D.; Theaker, J.; Guy, S. P.; Brown, T.; Little, S. *Nat. Biotechnol.* **1999**, *17*, 804−807.
(22) Talavera, E. M.; Afkir, M.; Salto, R.; Vargas, A. M.; Alvarez-Pez, J. M. *J. Photochem. Photobiol. B* **2000**, *59*, 9−14.
(23) Crockett, A. O.; Wittwer, C. T. *Anal. Biochem.* **2001**, *290*, 89−97.
(24) French, D. J.; Archard, C. L.: Brown, T.; McDowell, D. G. *Mol. Cell Probes* **2001**, *15*, 363−374.
(25) Vaughn, C. P.; Elenitoba-Johnson, K. S. J. *Am. J. Pathol.* **2003**, *163*, 29−35.
(26) Randolph, J. B.; Wagonner, A. S. *Nucleic Acids Res.* **1997**, *25*, 2923−2929.
(27) Misra, A.; Mishra, S.; Misra, K. *Bioconjugate Chem.* **2004**, *15*, 638−646.
(28) Yamana, K.; Iwase, R.; Furutani, S.; Tsuchida, H.; Zako, H.; Yamaoka, T. Murakami, A. *Nucleic Acids Res.* **1999**, *27*, 2387−2392.
(29) Yamana, K.; Zako, H.; Asazuma, K.; Iwase, R.; Nakano, H.; Murakami, A. *Angew. Chem. Int. Ed.* **2001**, *40*, 1104−1106.
(30) Yamana, K.; Iwai, T.; Ohtani, Y.; Sata, S.; Nakamura, M.; Nakano, H. *Bioconjuate Chem.* **2002**, *13*, 1266−1273.
(31) Korshun, V. A.; Stetsenko, D. A.; Gait, M. J. *J. Chem. Soc. Perkin Trans. 1* **2002**, 1092−1104.
(32) Mahara, A.; Iwase, R.; Sakamoto, T.; Yamana, K.; Yamaoka, T.; Murakami, A. *Angew. Chem. Int. Ed.* **2002**, *41*, 3648−3650.
(33) Fujimoto, K.; Shimizu, H.; Inouye, M. *J. Org. Chem.* **2004**, *69*, 3271−3275.
(34) Okamoto, A.; Kanatani, K.; Saito, I. *J. Am. Chem. Soc.* **2004**, *126*, 4820−4827.
(35) Dohno, C.; Saito, I. *ChemBioChem* **2005**, *6*, 1075−1081.
(36) Fluorescence brightness is defined as the product of the extinction coefficient at the applied excitation wavelength ϵ_{ex} and the fluorescence emission quantum yield Φ_F. Throughout this article the term "fluorescence brightness" describes the fluorescence over a wavelength range, i.e., the area of the emission spectra, whereas the term "fluorescence intensity" correlates to the level of fluorescence at a given wavelength.
(37) Singh, S. K.; Nielsen, P.; Koshkin, A. A.; Wengel, J. *Chem. Commun.* **1998**, 455−456.
(38) Obika, S.; Nanbu, D.; Hari, Y.; Andoh, J.; Morio, K.; Doi, T.; Imanishi, T. *Tetrahedron Lett.* **1998**, *39*, 5401−5404.
(39) Wengel, J. *Acc. Chem. Res.* **1999**, *32*, 301−310.
(40) Koshkin, A. A.; Singh, S. K.; Nielsen, P.; Rajwanshi, V. K. Kumar, R.; Meldgaard, M.; Olsen, C. E.; Wengel, J. *Tetrahedron* **1998**, *54*, 3607−3630
(41) We define a 2′-amino-LNA as an oligonucleotide containing one or more 2′-amino-2′-deoxy-2′-*N*,4′-*C*-methylene-β-D-ribofuranosyl monomer(s).
(42) Singh, S. K.; Kumar, R.; Wengel, J. *J. Org. Chem.* **1998**, *63*, 10035−10039.
(43) Sørensen, M. D.; Petersen, M.; Wengel, J. *Chem. Commun.* **2003**, 2130−2131.
(44) Hrdlicka, P. J.; Babu, B. R.; Sørensen, M. D.; Wengel, J. *Chem. Commun.* **2004**, 1478−1479.
(45) Babu, B. R.; Hrdlicka, P. J.; McKenzie, C. J.; Wengel, J. *Chem. Commun.* **2005**, 1705−1707.
(46) Wengel, J. *Org. Biomol. Chem.* **2004**, *2*, 277−280.
(47) Babu, B. R.; Sørensen, M. D.; Hansen, D. L.; Wengel, J. Manuscript in preparation.
(48) Supporting Information.

Table 1. Thermal Denaturation Temperatures (T_m Values) for Duplexes of **ON1**-**ON23** and DNA/RNA Complements[a]

		T_m (ΔT_m/mod)/°C	
		DNA	RNA
ON1	5′-GTG A***X***A TGC	30.5 (+2.5)	33.0 (+7.0)
ON2	5′-GCA ***X***AT CAC	34.0 (+6.0)	34.0 (+9.5)
ON3	5′-GCA TA***X*** CAC	32.5 (+4.5)	33.0 (+8.5)
ON4	5′-GCA ***X***A***X*** CAC	40.5 (+6.3)	41.5 (+8.5)
ON5	5′-GCA ***X***C***X*** CAC	49.0 (+7.0)	53.0 (+8.0)
ON6	5′-GCA ***X***G***X*** CAC	50.0 (+7.8)	51.5 (+9.0)
ON7	5′-GCA ***X***T***X*** CAC	38.0 (+4.3)	40.5 (+6.8)
ON8	5′-GTG ***X***TT TGC	30.0 (−1.5)	36.0 (+6.5)
ON9	5′-GTG ***X***T***X*** TGC	32.5 (+0.5)	41.0 (+5.8)
ON10	5′-GTG ***X***TT ***X***GC	33.5 (+1.0)	43.0 (+6.8)
ON11	5′-G***X***G ***X***T***X*** TGC	38.0 (+2.2)	51.0 (+7.2)
ON12	5′-GTG ***XX***T TGC	29.0 (−1.3)	37.5 (+4.0)
ON13	5′-GTG ***XXX*** TGC	24.0 (−2.5)	34.5 (+1.7)
ON14	5′-G***X***G ***XX***T ***X***GC	39.5 (+2.0)	53.0 (+5.9)
ON15	5′-TT***X*** A***X***A ***X***A***X*** CA^{Me}**C**^{L} G	58.0 (+5.6)[b]	62.5 (+7.1)[b]
ON16	5′-GTG ATA TGC	28.0[c]	26.0
ON17	5′-GCA TAT CAC	28.0[c]	24.5
ON18	5′-GCA TCT CAC	35.0	37.0
ON19	5′-GCA TGT CAC	34.5	33.5
ON20	5′-GCA TTT CAC	29.5	27.0
ON21	5′-GTG TTT TGC	31.5	29.5
ON22	5′-TTT ATA TAT CA^{Me}**C**^{L} G	35.5	34.0
ON23	5′-TT**T**^{L} AT^{L}A **T**^{L}AT^{L} CA^{Me}**C**^{L} G	52.5 (+4.3)[b]	60.5 (+6.6)[b]

[a] Thermal denaturation temperatures [T_m values/°C (ΔT_m/mod = change in T_m value per **X** modification calculated relative to DNA:DNA or DNA:RNA reference duplex)] measured as the maximum of the first derivative of the melting curve (A_{260} vs temperature) recorded in medium salt buffer ([Na^+]=110 mM, [Cl^-]=100 mM, pH 7.0 (NaH_2PO_4/Na_2HPO_4)), using 1.0 μM concentrations of the two complementary strands. T_m values are averages of at least two measurements; A = adenin-9-yl DNA monomer, C = cytosin-1-yl DNA monomer, G = guanin-9-yl DNA monomer, T = thymin-1-yl DNA monomer, **T**^{L} = thymin-1-yl LNA monomer, ^{Me}**C**^{L} = 5-methylcytosin-1-yl LNA monomer; see Figure 1 for structure of monomer **X** (the symbol "***X***" is used in the Table for clarity). [b] ΔT_m/mod value relative to **ON22**. [c] **ON16** and **ON17** are complementary.

plements (ΔT_m = +2.5 to +6.0 °C or +7.0 to +9.5 °C, respectively, relative to unmodified reference duplexes). The observed increases in thermal stability are similar to those observed with unprotected or N2′-methyl substituted 2′-amino-LNAs,[42] suggesting that the fluorophore moiety of monomer **X** is fully compatible with the structure of nucleic acid duplexes. Incorporation of an additional monomer **X** in this sequence context results in an approximately additive increase in thermal stability (T_m data of **ON4** relative to **ON2** and **ON3**). The nucleotide separating two **X** monomers was systematically varied to assess sequence specific effects on duplex formation (**ON4**-**ON7**). Comparable increases in thermal stability of duplexes with DNA (ΔT_m/mod = +6.3 to +7.8 °C) and RNA complements (ΔT_m/mod = +8.5 to +9.0 °C) are observed for probes where two **X** monomers are separated by A, C or G (**ON4**-**ON6**). Slightly lower increases are observed when T separates the **X** monomers (**ON7**). These results are in contrast to observations with DNA-probes containing O2′-pyrenylmethyl uridines, which only display strong stabilization toward DNA complements, and only if the 3′-flanking nucleotides are A or G.[28]

Surprisingly, incorporation of a single monomer **X** in a thymidine rich 9-mer-sequence context induces a slight decrease in thermal stability of the duplex with complementary DNA (ΔT_m = −1.5 °C), whereas an increase against complementary RNA (ΔT_m = +6.5 °C) is observed (compare T_m data for **ON8** relative to unmodified **ON21**). Incorporation of additional **X** monomers counteracts the destabilization against complementary DNA and results in additive increases in thermal stability toward RNA complements, provided that the **X** monomers are separated by one or two nucleotides (compare T_m data for **ON8** and **ON9**-**ON11**). The generally decreased stabilization in this sequence context relative to the mixed sequence 9-mers (**ON1**-**ON7**) may be a consequence of a distinct helical structure of the duplexes formed. N2′-substituents of 2′-amino-LNAs are known to point toward the minor groove,[43,44] and may therefore be affected by the narrow minor grooves in duplexes with A-tracts.[49] Relative destabilization toward DNA/RNA complements is observed upon sequential incorporation of two or three monomers **X** (compare T_m data for **ON8**, **ON12**, and **ON13**), suggesting that the minor groove becomes too crowded to accommodate the fluorophore moieties. This hypothesis is further verified by the absence of a cooperative melting transition for an almost fully modified 5′-**X**$_9$T sequence against DNA/RNA complements[43,50] and by molecular modeling of **ON13**:DNA (vide infra).

The Watson−Crick selectivity of singly and doubly modified pyrene-functionalized 2′-amino-LNA probes **ON1** and **ON4** was evaluated by measuring thermal denaturation temperatures of the corresponding complexes formed with DNA or RNA strands containing a single mismatched nucleotide in the central position. Excellent discrimination against mismatched DNA and RNA, which is at least comparable to unmodified DNA strands,[40] is observed for both probes (Table 2), suggesting that intercalation of pyrene moieties between nucleobases is not likely to explain the increased thermal stabilities of the duplexes formed between 2′-*N*-(pyren-1-yl)carbonyl-2′-amino-LNAs and DNA/RNA complements (Table 1).

Fluorescence Properties of 2′-*N*-(Pyren-1-yl)carbonyl-2′-amino-LNAs. Steady-state fluorescence emission spectra of 2′-*N*-(pyren-1-yl)carbonyl-2′-amino-LNAs and the corresponding duplexes with DNA or RNA complements, were recorded in thermal denaturation buffer using an excitation wavelength of 340 nm and equimolar quantities of each strand (applied concentration range ≈ 20−150 μM). Single stranded probes containing a single incorporation of monomer **X** display an unstructured band at λ_{max} ≈ 402 nm with a shoulder at λ_{max} ≈ 387 nm (shown for **ON2,** Figure 2). Upon hybridization with DNA/RNA complements two vibronic bands at λ_{max} ≈ 383 nm and λ_{max} ≈ 398 nm emerge and an approximately 2.5-fold increase in fluorescence intensity (measured at λ_{em} = 383 nm) is observed (Figure 2). Fluorescence emission quantum yields (Φ_F) of 2′-*N*-(pyren-1-yl)carbonyl-2′-amino-LNAs and their corresponding duplexes with DNA or RNA, were determined in thermal denaturation buffer at 19 °C relative to pyrenebutanoic acid in methanol (Φ_F = 0.065)[51] and 9,10-diphenylanthracene in cyclohexane (Φ_F = 0.95)[52] following standard procedures.[48,52] Deoxygenation was deliberately not applied to the samples since the scope of the work was to determine fluorescence enhancement under aerated conditions prevailing in various bioassays. However, the effect of argon purging of selected samples turned out to be negligible.[48] The quantum yield of fully deprotected 2′-*N*-(pyren-1-yl)carbonyl-2′-amino-LNA nucleoside **2**[47] (Figure 1), was determined to be Φ_F =

(49) Woods, K. K.; Maehigashi, T.; Howerton, S. B.; Sines, C. C.; Tannenbaum, S.; Williams, L. D. *J. Am. Chem. Soc.* **2004**, *126*, 15330−15331.
(50) The corresponding LNA-T (**T**^{L}) sequence, 5′-(**T**^{L})$_9$T, has thermal denaturation temperatures of 80.0 °C and 70.5 °C against DNA and RNA complements, respectively.[37]
(51) Netzel, T. L.; Nafisi, K.; Headrick, J.; Eaton, B. E. *J. Phys. Chem.* **1995**, *99*, 17948−17955.
(52) Morris, J. V.; Mahaney, M. A.; Huber, J. R. *J. Phys. Chem.* **1976**, *80*, 969−974.

Table 2. Selectivity of **ON1** and **ON4** toward Complementary or Singly Mismatched DNA/RNA[a]

			T_m/°C							
			DNA				RNA[b]			
		B:	A	C	G	T	A	C	G	U
ON1 target	5′-GTG A***X***A TGC 3′-CAC T**B**T ACG		**30.5**	< 10	< 10	15.5	**33.0**	< 10	15.0	18.5
target **ON4**	5′-GTG A**B**A TGC 3′-CAC ***X***A***X*** ACG		19.5	25.0	23.0	**40.5**	27.0	26.0	31.0	**41.5**

[a] For conditions of thermal denaturation experiments, see Table 1. T_m values of fully matched duplexes are shown in bold. [b] The target sequence contains U instead of T.

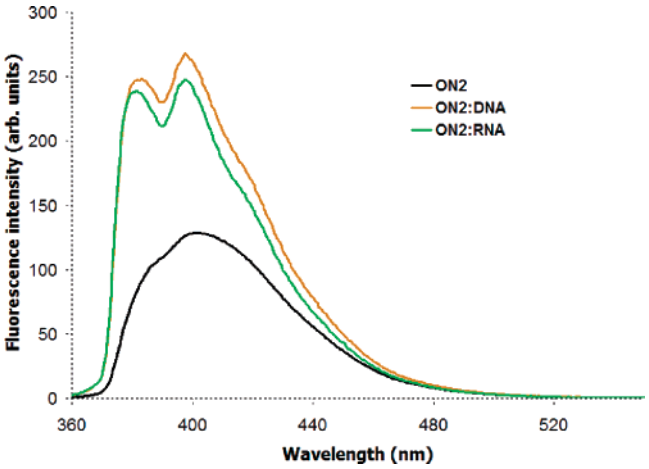

Figure 2. Steady-state fluorescence emission spectra of **ON2** and the corresponding duplexes with DNA/RNA complements. Spectra were recorded in thermal denaturation buffer (see Table 1) at 19 °C using an excitation wavelength of 340 nm and are normalized with respect to ON concentration.

0.34 in aerated thermal denaturation buffer.[53] Usually, fluorescence quantum yields of pyrene derivatives drop considerably upon incorporation into ONs acids due to quenching by neighboring nucleobases.[54] However, duplexes of **ON1**-**ON3** and complementary DNA/RNA exhibit remarkably high fluorescence quantum yields of $\Phi_F = 0.77-0.79$ and $\Phi_F = 0.79-0.91$, respectively (Table 3), which compare very favorably with state-of-the-art pyrene-labeled probes, which display fluorescence quantum yields of up to $\Phi_F \approx 0.24$.[28,34−35] It is noteworthy that increases in fluorescence brightness are observed upon binding to DNA as well as to RNA complements, considering that ONs containing O2′-pyrenylmethyl ether[28,29] or carbamate[31] derivatives of uridine only display significant increases in fluorescence brightness upon hybridization to RNA.

Interestingly, duplexes of doubly modified **ON4** and DNA/RNA complements exhibit approximately additive increases in fluorescence brightness[36] (FB = $\epsilon_{340} \times \Phi_F$) compared to the corresponding duplexes of singly modified probes, since fluorescence quantum yields remain unchanged and an additive increase in the extinction coefficient ϵ_{340} is observed (Table 3).

Next, the nucleotide separating two **X** monomers was varied systematically (**ON4**-**ON7**, Table 3) since neighboring nucleotides are known to quench fluorescence of pyrene substituents to different extent.[54] The fluorescence brightness of duplexes between probes and DNA complements decreases in the order **ON4** > **ON6** > **ON7** > **ON5**, whereas the order is **ON4** > **ON7** > **ON6** > **ON5** with RNA complements. The low fluorescence brightness of duplexes between **ON5** and DNA or RNA are due to the low extinction coefficients ($\epsilon_{340} = 21$ $mM^{-1}\cdot cm^{-1}$) of the **X**C**X**-sequence context (compare ϵ_{340} data for **ON4**−**ON7**, Table 3).[55] The reasons for the decreased extinction coefficients are unknown. Duplexes of **ON7** and DNA or RNA complements display slightly lower fluorescence quantum yields ($\Phi_F \approx 0.6$) than the corresponding duplexes with **ON4**-**ON6**. Nonetheless, the sequence dependency of fluorescence quantum yields and intensities is significantly lower than, e.g., for the related O2′-pyrenylmethyl uridine containing DNA-probes.[28]

It is noteworthy, that fluorescence quantum yields of unhybridized doubly modified probes **ON4**-**ON7** are significantly lower than for singly modified probes **ON1**-**ON3** (Table 3),[56] and thus larger hybridization-induced increases in fluorescence intensity and brightness[36] are observed (compare FB data for **ON1**-**ON3** and **ON4**-**ON7**, Table 3). As an example, approximately eight- and eleven-fold increases in fluorescence intensity at $\lambda_{em} = 383$ nm are observed upon hybridization of **ON7** to DNA or RNA complements, respectively (Figure S6).[48]

The relative positions of monomers **X** were varied in a T-rich 9-mer sequence context to determine the effect of the distance between two monomers **X** on the fluorescence properties of 2′-*N*-(pyren-1-yl)carbonyl-2′-amino-LNAs (Table 3). The steady-state fluorescence emission spectra of singly modified **ON8** and its corresponding duplexes with DNA/RNA complements (data not shown) resemble the corresponding spectra of the singly modified probes in the mixed sequence context (**ON1**-**ON3**), although fluorescence quantum yields and intensities generally are slightly lower (Table 3). Duplexes of multiple modified probes and DNA/RNA complements also exhibit approximately additive increases in fluorescence brightness in this sequence context as long as monomers **X** are separated by at least one nucleotide (compare data for **ON8**-**ON11**:DNA/RNA, Table 3). There are no significant differences in the fluorescence properties of duplexes between probes with one or two nucleotides, respectively, separating two **X** monomers and DNA/RNA

(53) Area vs A_{340} curves of pyrenebutanoic acid in methanol for calibration of emission quantum yield measurements and of unprotected nucleoside **2** in thermal denaturation buffer for determination of emission quantum yield are shown in Supporting Information (Figure S5).[48]

(54) Manoharan, M.; Tivel, K. L.; Zhao, M.; Nafisi, K.; Netzel, T. L. *J. Phys. Chem.* **1995**, *99*, 17461−17472.

(55) A comparison of the extinction coefficients of **ON3** with those of **ON1** or **ON2**, indicates that the presence of a 3′-flanking C does not lead to a decrease in extinction coefficient. Thus, the decreased ϵ_{340} value of **ON7** may be due to the 5′-flanking C.

(56) **ON4** exhibits the brightest fluorescence among the single stranded doubly modified probes **ON4**-**ON7**. The thermal denaturation temperature of **ON4** was determined to investigate whether the fluorescence is caused by self-hybridization of the central A**X**A**X**-segment. Indeed, a thermal denaturation temperature of 22.0 °C was observed for single stranded **ON4**, but only a slight decrease in quantum yield was observed when the steady-state fluorescence emission spectrum was recorded at 35 °C instead of at 19 °C (not shown).

Table 3. Quantum Yields, Extinction Coefficients and Fluorescence Brightness for Single Stranded Probes **ON1**-**ON15** and the Corresponding Complexes with DNA/RNA Complements in Aerated Thermal Denaturation Buffer at 19 °C.[a]

		Φ_F			ϵ_{340}/ $mM^{-1}\cdot cm^{-1}$			FB		
		SSP	DNA	RNA	SSP	DNA	RNA	SSP	DNA	RNA
ON1	5′-GTG A***X***A TGC	0.47	0.77	0.79	20	16	15	9.4	12.3	11.9
ON2	5′-GCA ***X***AT CAC	0.38	0.79	0.88	24	22	19	9.1	17.4	16.7
ON3	5′-GCA TA***X*** CAC	0.50	0.79	0.91	20	20	17	10	15.8	16.7
ON4	5′-GCA ***X***A***X*** CAC	0.27	0.81	0.70	50	45	45	13.5	36.5	31.5
ON5	5′-GCA ***X***C***X*** CAC	0.05	0.56	0.84	nd	21	21	nd	11.8	17.6
ON6	5′-GCA ***X***G***X*** CAC	0.05	0.62	0.71	nd	42	36	nd	26.0	25.6
ON7	5′-GCA ***X***T***X*** CAC	0.09	0.55	0.62	37	37	45	3.3	20.7	27.9
ON8	5′-GTG ***X***TT TGC	0.10	0.34	0.40	23	26	34	2.3	8.8	14
ON9	5′-GTG ***X***T***X*** TGC	0.04	0.28	0.55	47	46	50	1.9	13	28
ON10	5′-GTG ***X***TT ***X***GC	0.05	0.41	0.50	42	48	51	2.1	20	26
ON11	5′-G***X***G ***X***T***X*** TGC	0.04	0.35	0.68	62	66	77	2.5	23	52
ON12	5′-GTG ***XX***T TGC	0.02	0.04	0.09	60	64	64	1.2	2.6	5.8
ON13	5′-GTG ***XXX*** TGC	0.02	0.02	0.07	74	45	52	1.5	0.9	3.6
ON14	5′-G***X***G ***XX***T ***X***GC	0.06	0.07	0.11	106	74	84	6.4	5.2	9.2
ON15	5′-TT***X*** A***X***A ***X***A***X*** CA^{Me}**C**^{L} G	0.05	0.99	0.96	64	51	60	3.2	51	58

[a] Extinction coefficients ϵ_{340} determined at $\lambda = 340$ nm and fluorescence brightness FB in $mM^{-1}\cdot cm^{-1}$ calculated as: $FB = \Phi_F \times \epsilon_{340}$, SSP denotes a single stranded probe, nd means not determined, see Figure 1 for structure of monomer **X** (the symbol "***X***" is used in the Table for clarity).

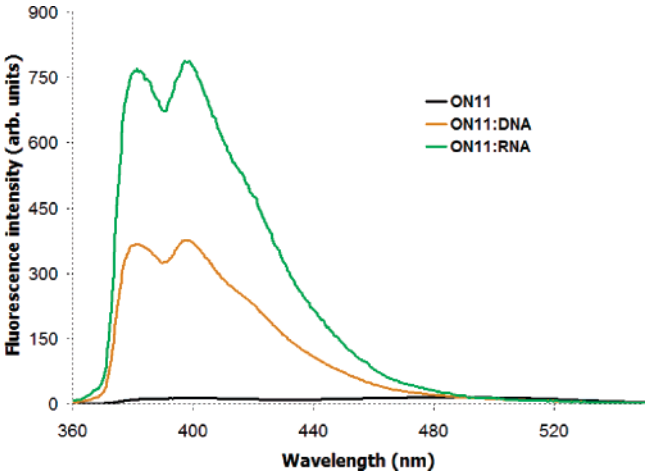

Figure 3. Steady-state fluorescence emission spectra of **ON11** and the corresponding duplexes with complementary DNA/RNA. For conditions see Figure 2.

complements (compare data for **ON9** and **ON10**). The approximately additive extinction coefficients and constantly large fluorescence quantum yields observed for duplexes with high labeling density, are remarkable considering the problems observed with other multiple fluorophore-labeled ONs.[26] The fluorescence of single stranded multiple labeled **ON9**−**ON11** is efficiently quenched ($\Phi_F \approx 0.05$), thus reinforcing multiple incorporations as a means to enhance the sensitivity of DNA/RNA detection. This is demonstrated by the very large increases in fluorescence intensity at $\lambda_{em} \approx 383$ nm observed upon binding of **ON11** to DNA/RNA complements (33-fold and 69-fold increases, respectively, Figure 3).

Conversely, the fluorescence emission spectra of duplexes formed between probes containing two or three sequential incorporations of monomer **X** and DNA/RNA complements are unstructured (data not shown) and exhibit very low quantum yields and fluorescence brightness (data for **ON12** and **ON13**, Table 3). Excimer emission was not observed, neither in single stranded **ON12** and **ON13** nor in their duplexes with DNA/RNA complements. These fluorescence properties, along with the observed decreased thermal stability of the duplexes (Table 1), suggest that a distorted duplex geometry is adopted upon sequential incorporation of **X** monomers. Interestingly, a probe with four incorporations of monomer **X** (two sequential and two separated, **ON14**, Table 3), exhibits very low fluorescence intensity while retaining high thermal stability toward DNA and RNA complements (Table 1).

Fluorescence emission spectra of **ON4** and mismatched DNA-targets recorded at 19 °C, i.e., close to the denaturation temperatures of the mismatched complexes (Table 2) closely resemble spectra of single stranded **ON4** both in terms of shape and intensity (Figure S7, $\Phi_F = 0.31-0.35$).[48] Conversely, relatively bright fluorescence was observed at 19 °C ($\Phi_F = 0.47-0.52$) upon hybridization of **ON4** to mismatched RNA-targets (Figure S8 − upper panel).[48] Upon raising the temperature of the experiment to 30 °C, quantum yields and thus fluorescence intensities (at $\lambda_{em} = 383$ nm) of the mismatched complexes dropped significantly. In comparison, the quantum yield of the fully matched **ON4**:RNA duplex decreased only slightly at this temperature ($\Phi_F \approx 0.58$) (Figure S8−lower panel).[48] Apparently, a mismatch-induced distortion in duplex geometry does not weaken the fluorescence intensity. However, these proof-of-principle experiments illustrate, that the excellent Watson−Crick mismatch selectivity of monomer **X** can be used to ascertain hybridization under stringent conditions for generation of specific signals, either by controlling the temperature or by appropriate sequence design for in vivo applications.

Detection Limits. Collectively, the observations described above suggest that probes with two or more separated **X** monomers (1) form very stable duplexes with complementary DNA/RNA, (2) lead to large hybridization-induced increases in fluorescence intensity and (3) generate brightly fluorescent duplexes with DNA/RNA complements. To verify these conclusions and to explore detection limits, four separated **X** monomers were incorporated in a 13-mer TA-rich sequence context (**ON15**). As expected a large increase in binding affinity toward DNA/RNA complements relative to reference sequence **ON22** and a small increase relative to the corresponding LNA sequence **ON23** were observed (Table 1). Moreover, approximately 23-fold hybridization-induced increases in fluorescence intensity (at $\lambda_{em} = 383$ nm) (**ON15**, see also Table 3 for fluorescence brightness data) were observed. This is particularly encouraging considering that much smaller increases were observed for the doubly modified probe **ON4** having a similar sequence context.

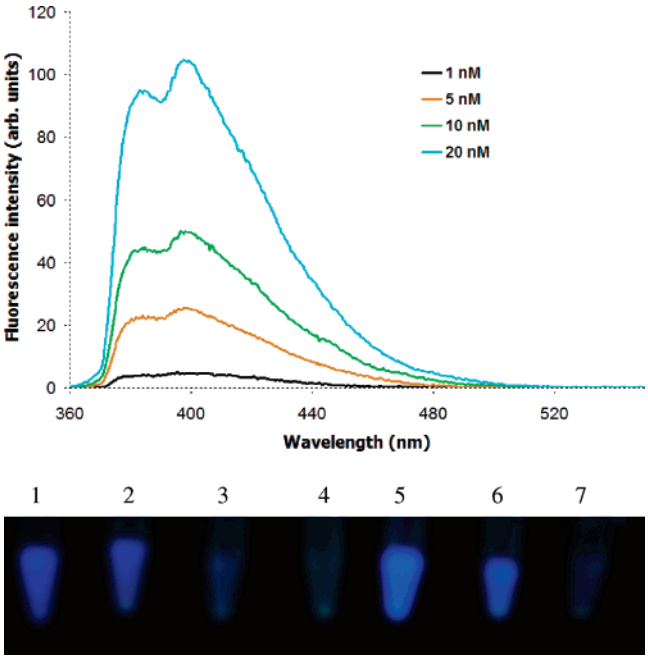

Figure 4. Detection limits. Upper panel: steady-state fluorescence emission spectra of **ON15** and RNA complement using 1−20 nM concentration. Lower panel: **ON15** and DNA complement each at 1 μM, 500 nM, and 100 nM concentration (vial 1−3), thermal denaturation buffer (vial 4, negative control) and **ON15** and RNA complement each at 1 μM, 500 nM, and 100 nM concentration (vial 5−7). Volume in each vial is 200 μL. Samples were illuminated using a standard laboratory UV-lamp, $\lambda_{ex} = 365$ nm. Photographs were taken with a standard digital camera.

Even more remarkably, the quantum yields of duplexes between **ON15** and DNA/RNA complements approached unity and the duplexes were easily detectable at concentrations down to 5 nM using a standard luminescence spectrometer at nonoptimized conditions (Figure 4−upper panel).[48] Illumination of these duplexes by a standard laboratory lamp used for visualization of TLC-plates ($\lambda_{ex} = 365$ nm), allowed detection of these duplexes at concentrations down less than 500 nM by the naked eye (Figure 4−lower panel).

Rationalization of Fluorescence Properties. An explanation for the fluorescence quenching of single stranded probes containing separated **X** monomers when compared to the corresponding duplexes with DNA/RNA complements, may be inferred from the fluorescence emission spectra. The relative intensities of the vibronic bands I and III are sensitive to the polarity in the microenvironment—higher I_{III}/I_I-ratios are observed in apolar environments.[57] The single stranded probes **ON1**-**ON7** exhibit an I_{III}/I_I-ratio (measured as the intensities at $\lambda_{em} = 383$ and 398 nm) of approximately 1.3−1.4, whereas the ratio drops to 1.0−1.1 upon hybridization to DNA/RNA complements. This suggests that the flexible single stranded probes can fold up and allow pyrene moieties to interact with the hydrophobic nucleobases and thereby promote quenching of fluorescence. Hybridization to DNA/RNA complements leads to formation of a rigid double helix in which the pyrene moieties are positioned in the more polar minor groove, where it is unsymmetrically surrounded by partial charges. Hybridization-induced increases in fluorescence intensity observed with DNA probes containing C4′-pyrenecarboxamidemethyl-modified thymidines,[35] or fluorescein labeled HyBeacons[58] or with DNA[28] or RNA probes[29] containing O2′-pyrenylmethyl uridine, have been explained in a similar manner. Simple force field calculations of **ON4**:DNA, using the Amber force field[59] as implemented in MacroModel V7.2,[60] substantiate this hypothesis. In the lowest energy structure of **ON4**:DNA, the pyrene moieties of monomers **X** are positioned at the brim of the minor groove as expected,[43,44] and are wedging into the groove while following the curvature of the double helix (Figure 5). The carbonyl group of the amide bond is oriented toward the edge of the minor groove, where it may coordinate with solvent molecules. The dioxabicyclo[2.2.1]heptane skeleton of monomer **X** renders the sugar moiety in a rigid North conformation and in concert with the amide linkage, restricts movement of the pyrene moiety in the minor groove as long as **X** monomers are separated.[61] Interactions between pyrene moieties and nucleobases, which could lead to quenching of fluorescence are thereby reduced. We speculate that the increased fluorescence quenching of unhybridized probes containing two or more separated **X** monomers, when compared to singly modified probes such as **ON1**-**ON3**, may originate from interactions between excited and ground-state pyrenes which do not, however, lead to observable excimer emission due to constraints imposed by the three-dimensional structure.[62]

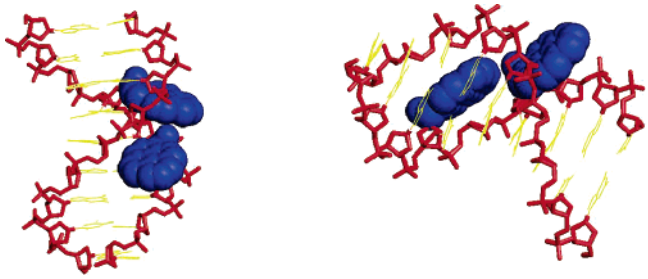

Figure 5. Two representations of the lowest energy structure of **ON4**:DNA. For clarity hydrogens, sodium ions and bond orders have been omitted. Coloring scheme: nucleobases, yellow; sugar−phosphate backbone, red; pyren-1-yl-carbonyl moiety, blue.

A comparison of the lowest energy structures of **ON4**:DNA (Figure 3) and **ON13**:DNA (Figure S9),[48] the latter containing three sequentially incorporated **X** monomers, reveals interesting differences in the positioning of the pyrene moieties in the minor groove. Two pyrene moieties can adopt conformations that bring them significantly closer to each other in **ON13**:DNA (shortest C−C distance, ~3.4 Å) than in **ON4**:DNA (~6.0 Å). Also, the two torsion angles Ψ_1 (C2′−N2′−C═O) and Ψ_2 (N2′−C(O)−$C1_{pyr}$−$C2_{pyr}$) of the three pyrene moieties of **ON13**:DNA differ significantly among each other ($\Psi_1 = 22°$, 129°, and 128° and $\Psi_2 = 117°$, −53°, and −31°, for the three monomers **X** listed from 5′- to 3′-end, respectively) and when compared to **ON4**:DNA ($\Psi_1 \approx 176°$ and $\Psi_2 \approx -64°$, for both monomers). These

(57) Kalyanasundaram, K.; Thomas, J. K. *J. Am. Chem. Soc.* **1977**, *99*, 2039−2044.
(58) Marks, A. H. R.; Bhadra, P. K.; McDowell, D. G.; French, D. J.; Douglas, K. T.; Bichenkova, E. V.; Bryce, R. A. *J. Biolmol. Struct. Dyn.* **2005**, *23*, 49−62.
(59) Weiner, S. J.; Kollmann, P. A.; Case, D.; Singh, U. C.; Ghio, C.; Alagona, G.; Profeta, S.; Weiner, P. K. *J. Am. Chem. Soc.* **1984**, *106*, 765−784.
(60) Mohamadi, R. D.; Richards, N. G: J.; Guida, W. C.; Liskamp, R.; Lipton, M.; Caufield, C.; Chang, C.; Hendrickson, T.; Still, W. C. *J. Comput. Chem.* **1990**, *11*, 440−467.
(61) The ratio between rotamers when 2′-*N*-(pyren-1-yl)carbonyl-2′-amino-LNA monomer **X** is incorporated in an ON is unknown. However, it should be noted that the duplexes are denatured by heating followed by reannealing prior to recording thermal denaturation curves (displaying smooth single transitions) or steady-state fluorescence spectra.
(62) Winnik, F. M. *Chem. Rev.* **1993**, *93*, 587−614.

results suggest that the minor groove of a standard B-type double helix may be too narrow to accommodate sequentially incorporated **X** monomers. Distortions of the helix geometry must therefore be expected (helix is kept rigid during calculations), which is in accordance with the T_m data for **ON12**:DNA and **ON13**:DNA (Table 1). The mechanism of fluorescence quenching may be similar to that proposed for single stranded probes, i.e., local distortions of the duplex geometry may increase interactions between pyrene moieties and nucleobases or between two pyrene moieties, whereby fluorescence is quenched. To further investigate these observations, ongoing work focuses on determining fluorescence lifetimes of single stranded probes and their corresponding duplexes with DNA/RNA complements.

Conclusion

Development of more sensitive probes for detection of nucleic acids in homogeneous fluorescence assays is desirable.[63] Herein, 2′-*N*-(pyren-1-yl)carbonyl-2′-amino-LNAs have been demonstrated to be very promising probes due to:

- Large increases in thermal stability upon hybridization to DNA/RNA complements with excellent Watson−Crick mismatch discrimination as compared to unmodified reference duplexes,
- Very bright, virtually sequence-independent, fluorescence for duplexes of probes and DNA/RNA complements with emission quantum yields of magnitudes ($\Phi_F = 0.30-0.99$) which are unprecedented among pyrene-labeled nucleic acids,
- Large hybridization-induced increases (up to 69-fold) in fluorescence intensity if two or more separated **X** monomers are incorporated in oligodeoxyribonucleotides.

Molecular modeling and fluorescence studies suggest that the dioxabicyclo[2.2.1]heptane skeleton and amide linkage of 2′-*N*-(pyren-1-yl)carbonyl-2′-amino-LNA monomer **X** fix the position of the pyrene moiety in the minor groove of nucleic acid duplexes, whereby interactions between the pyrene moiety and nucleobases, typically leading to quenching of fluorescence, are reduced. Thus, attachment of fluorophores to the N2′-position of 2′-amino-LNA via short amide linkages may become a general paradigm for tethering of fluorophores to oligonucleotides without the typical loss in fluorescence intensity. A particularly interesting application of pyrene-functionalized 2′-amino-LNA probes will be real-time in vivo imaging of RNA—especially in light of the known stability of LNAs to 3′-exonucleases and 3′-endonucleases and lack of RNase H catalyzed fragmentation of mixmer LNA:RNA complexes.[64]

Acknowledgment. We greatly appreciate funding from The Danish National Research Foundation and The Danish Research Agency. Moreover, we acknowledge financial support within the frame of the program: Control of assembly and charge transport dynamics of immobilized DNA (CIDNA) − A specific targeted research project within the sixth framework program of the EC, priority: NMP − Nanotechnology and nanoscience, knowledge based multifunctional materials, new production processes and devices, proposal no. 505669-1. Ms. B. M. Dahl, University of Copenhagen and Dr. M. Meldgaard, Exiqon A/S, are thanked for oligonucleotide synthesis and MALDI−MS analysis, respectively. We sincerely value the technical assistance of Ms. K. Østergaard and Ms. S. W. Lena, University of Southern Denmark.

Supporting Information Available: Experimental protocols for thermal denaturation studies, fluorescence steady-state emission studies, quantum yield determinations, and molecular modeling studies as well as MALDI−MS of synthesized ONs (Table S1), representative thermal denaturation curves (Figures S1−S4), Area vs A_{340} calibration curve of pyrenebutanoic acid in methanol for fluorescence quantum yield measurements (Figure S5 − upper panel), Area vs A_{340} curve for determination of quantum yield of unprotected nucleoside **2** in thermal denaturation buffer (Figure S5 − lower panel), steady-state fluorescence emission spectra of **ON7** and complementary DNA/RNA targets (Figure S6), steady-state fluorescence emission spectra of **ON4** and complementary or mismatched DNA (Figure S7) or RNA targets (Figure S8) and lowest energy modeling structure of **ON13**:DNA (Figure S9). This material is available free of charge via the Internet at http://pubs.acs.org.

JA052887A

(63) For a very recent review on fluorescence-based detection of cellular RNAs, see: Silverman, A. P.; Kool, E. T. *Trends Biotechnol.* **2005**, *23*, 225−230.

(64) Petersen, M.; Wengel, J. *Trends Biotechnol.* **2003**, *21*, 74−81.